

## Intercepted rainfall in *Abies fabri* forest with different-aged stands in southwestern China

Xiangyang SUN<sup>1,2,3</sup>, Genxu WANG<sup>1,2,\*</sup>, Yun LIN<sup>4</sup>, Linan LIU<sup>1,2,3</sup>, Yang GAO<sup>1,2,3</sup>

<sup>1</sup>Institute of Mountain Hazards and Environment, Chinese Academy of Sciences, Chengdu 610041, P.R. China

<sup>2</sup>Key Laboratory of Mountain Environment Evolution and Regulation, Institute of Mountain Hazards and Environments, Chinese Academy of Sciences, Chengdu 610041, P.R. China

<sup>3</sup>Graduate University of Chinese Academy of Sciences, Beijing 100049, P.R. China

<sup>4</sup>Institute of Resources & Environment, Henan Polytechnic University, Jiaozuo 454003, P.R. China

Received: 17.07.2012 • Accepted: 05.12.2012 • Published Online: 16.07.2013 • Printed: 02.08.2013

**Abstract:** Interception is one of the most important hydrological processes. Most investigations merely focus on canopy interception, but forest floor interception should also be considered. The stand age also influences interception. To explore the interception characteristics of *Abies fabri* with different stand ages, canopy, stem, and forest floor, interceptions were evaluated during the rainy season of 2009 (from May to October 2009). The total interception rates were found to be 28.8%, 25.5%, and 31.3% for young, middle-aged, and mature forest stands, respectively. Forest floor interception accounted for 19.1%, 18.1%, and 10.0% of the total interception, respectively. We concluded that the differences among the interceptions of the forest stands were correlated with the leaf area index. A higher stand height also reduced the rate of forest floor evaporation. The water-storage capacities of the young, middle-aged, and mature forest stands were 8.22, 7.61, and 10.78 mm, respectively. These results implied that the canopy and forest floor interceptions were related to the forest water balance, and that accurate estimates of the interception of different-aged forest stands were crucial in evaluating the role of a forest in the hydrological cycle.

**Keywords:** *Abies fabri*, Gongga Mountain, intercepted rainfall, stand age

### 1. Introduction

Rainfall interception by the forest ecosystem and its evaporation to the atmosphere is a major component of the water balance (Savenije 2004; Miralles et al. 2011). At the global land-surface scale, transpiration, interception loss, bare soil evaporation, and snow sublimation contribute to 80%, 11%, 7%, and 2% of the total evaporation, respectively. Rainfall interception plays an important role in the partition of precipitation into evaporation and water available for runoff at a continental scale (Miralles et al. 2011). Rainfall interception differs among stand ages (Helvey 1967; Barbier et al. 2009), and the results of different studies are inconsistent (Murakami et al. 2000; Vertessy et al. 2001). Forest interception consists of 3 components: canopy, stem, and forest floor interceptions (Kubota et al. 2004; Gerrits et al. 2010). Interception is one of the most underrated and underestimated processes in rainfall-runoff analysis (Savenije 2004).

Water that evaporates from a wet canopy accounts for a considerable part of the interception loss because a canopy has an aerodynamically “rough” surface that is conducive to the turbulent transfer of water vapor away from the surface (Blyth and Harding 2011). Turbulent

diffusion above forests is much more efficient and potential evaporation from intercepted water exceeds open water evaporation (Shuttleworth 1993). The throughfall ( $T_p$ ) is the proportion of incident gross precipitation that drips to the ground. The stemflow ( $S_p$ ) is the proportion that runs down the stems to the ground. The canopy interception ( $I_c$ ) is obtained by subtracting the sum of the throughfall and stemflow from the gross rainfall (Mair et al. 2010). The canopy interception rate is approximately 25%–50% of the precipitation in coniferous forests (Rutter et al. 1975; Gash et al. 1980; Johnson 1990) and 10%–35% of that in broad-leaved forests (Rutter et al. 1975; Rowe 1983). The percentage of the interception to evapotranspiration ranges from 25% to 75% (Schellekens et al. 2000; David et al. 2006; Lawrence et al. 2007). If evaporation from interception is defined as the fast feedback to the atmosphere (within the time span of about 1 day) of rainfall that does not reach the root-zone or the drainage system, then interception has more contribution (Savenije 2004).

Stem interception is the part of rainfall that is intercepted by epiphytes (mosses, liverworts, and lichens, among others) and rough barks (Levia and Frost 2003). Epiphytes impede the drainage of water from the branch.

\* Correspondence: wanggx@imde.ac.cn

The turnover rates of water in the epiphyte mass are low (Veneklaas et al. 1990). Therefore, the canopy requires more rainfall to become saturated, delaying the saturation of the canopy (Schellekens et al. 2000; Pypker et al. 2006). Interception by epiphytes can reach a maximum water storage of 0.81 mm at stand level in montane tropical rain forests (Hölscher et al. 2004). The rainfall interception effect of epiphytes is determined by water content (Veneklaas et al. 1990) and epiphyte type (Fleischbein et al. 2005).

The forest floor can intercept a significant amount of throughfall (Gerrits et al. 2010). Forest floor interception affects runoff amounts, protects soils from erosion, and contributes to the stability of soil characteristics (Marin et al. 2000). Forest floor interception is often not considered in water balance studies because it is thought to be negligible. However, previous studies found that forest litter interception accounts for 12% of the annual rainfall in a savannah ecosystem (Tsiko et al. 2012), and that 22% of throughfall is intercepted by forest floor litter in a beech forest (Gerrits et al. 2010). The ratio of the forest floor evaporation to the total evaporation can vary due to forest cutting or thinning (Hattori 1983; Merta et al. 2006). Merta et al. (2006) found that soil surface evaporation considerably varies (from 50% to 1.5% of the total evaporation) with increased leaf area index (LAI) from 0.5 to 3.0 in a crop. Energy and water balance methods are used to study forest floor evaporation (Tajchman 1972; Gerrits et al. 2010; Tsiko et al. 2012). However, the results of these methods are mostly potential rather than actual evaporation rates because humidity is higher in microlysimeters than in surrounding soils (Kubota et al. 2004). Stable isotopes prove to be an effective approach for investigating the rate of forest floor evaporation (Kubota et al. 2004; Lin et al. 2011).

The *Abies fabri* forest is a typical subalpine dark coniferous forest in southwestern China. In our study area, young, middle-aged, and mature forests represent the different stand ages of *A. fabri*. The effects of *A. fabri* on hydrological processes largely remain unquantified. To understand clearly the interception characteristics of different-aged *A. fabri* forests under current climate conditions, in situ measurements and rainfall simulator experiments were performed to study canopy and stem interceptions. The oxygen-18 ( $\delta^{18}\text{O}$ ) was used to study forest floor litter interception. Our aims were to determine the amounts of interception components for the successive series of *A. fabri* and to investigate the variation in the interception capacities of the different components under different stand ages during the growing season (from May to October).

## 2. Materials and methods

### 2.1. Site description

Mt. Gongga (29°20'–30°20'N, 101°30'–102°15'E) is located on the transitional area between the eastern

monsoon subtropics of China and the frigid area of the Tibetan Plateau. It is the summit of Hengduan Mountain. The highest altitude of Mt. Gongga is 7556 m above sea level. The climate is dominated by the southeastern Pacific monsoon. The annual mean air temperature in this region is 3.9 °C. The annual rainfall is 1940 mm, with most rainfall concentrated from May to October, which accounts for 79.7% of the annual rainfall. The relative humidity during the wet season is 91%. The rainfall from May to October amounted to 1429 mm in 2009, which accounted for about 79.0% of the annual rainfall. Rainfall events were mainly of less than 20 mm during our study period, and the proportion was approximately 88.3%. About 90.8% of the duration of rainfall events ranged between 0 h to 20 h. The rainfall intensity in our study area was largely less than 1.5 mm/h. The rainfall rate at night was about 66.0%, which implied that more rainfall events occurred in the evening.

The wide altitude range (1100–7556 m) results in a vertically diverse range of vegetation zones, with forest types varying from subtropical to cold alpine vegetation zones. Our research area mainly consists of *A. fabri* and *Populus purdomii*. Young and middle-aged *A. fabri* regrew from where the original primeval *A. fabri* was destroyed by debris flows. During the growing period, *P. purdomii* continued to thin until *A. fabri* became the dominant middle-aged and mature forests. The mature stand grows in the soil of slope deposits, whereas the young and the middle-aged stands grow in moraine soil. The LAI was the mean value observed from May to October using an LAI-2000 (Li-Cor Bioscience, USA). Further details of these stands are given in Table 1. The soil is the mountain dark brown soil, which has high sand content and strong permeability.

**Table 1.** Characteristics of the stands of the forest in our study area.

	Mature	Middle-aged	Young
Area (m <sup>2</sup> )	100 × 50	30 × 40	30 × 40
Stand age (a)	100–120	70–80	30–40
Species	<i>A. fabri</i>	<i>A. fabri</i>	<i>A. fabri</i> , <i>P. purdomii</i>
Number (trees)	47	124	193
Height (m)	27.0	16.0	11.5
DBH (cm)	28.14	19.56	12.0
Slope (°)	15	12	5–10
Aspect	NW20°	SW70°	-
LAI	10.2*	7.8*	8.0†

Note: LAI marked with \* means that the value is from Luo et al. (2004), whereas those marked with † means that the values were measured using an LAI-2000 (LI-COR).

## 2.2. Rainfall measurements

Gross precipitation was routinely measured using an automatic meteorological observation system (AMOS; MILOS520, Vaisala Co., Finland). The AMOS also recorded other meteorological data, such as air temperature, wind speed, radiation, air temperature, and humidity. The AMOS was located at the Alpine Ecosystem Observation and Experiment Station of Mt. Gongga (submitted to CERN, China). Its air-line distances to the young, middle-aged, and mature forest observation plots were all within 300 m. Thus, we think that the observed meteorological data can represent the entire study area.

## 2.3 Throughfall measurements

The throughfall was measured using large stationary V-shaped troughs. We installed 4, 3, and 3 troughs at the young, middle-aged, and mature forest sites, respectively. An additional trough was installed for the young forest site because the forest in this area constituted 2 forest types. Each trough was 305 cm long, 24 cm wide, and 25 cm deep (equivalent to the deployment of 23.3 standard 200-mm-wide rain gauges). All troughs were installed at a slope of 15°, and the throughfall collected automatically flowed into the rain gauges through rubber pipes. Each trough was equipped with a rain gauge comprising 2 automatic tipping buckets, and data were recorded by loggers (CR2-J, Tongshu Technology Inc., China). The troughs were positioned 1.5 m above the ground to prevent contamination with rainfall splashing from ground. The gauges were calibrated so that the large tipping bucket collected 1.02 mm of rainfall for each tipping and the small tipping bucket collected 0.20 mm per tipping. The measured rainfall was calibrated by comparing with the actual rainfall, and the result showed that our rain gauges can capture the rainfall rate with an  $R^2$  value of 0.94 (1:1 line). The throughfall data were continuously stored at 1 h time intervals. The throughfall value at each experimental plot was expressed as the mean value of all troughs.

For calculation convenience, the throughfalls collected by the troughs were converted to rainfall depth using the following equation:

$$r = \frac{r_1 \cdot \pi d^2}{4A} \quad (1)$$

where  $r$  is the real throughfall depth (mm),  $r_1$  is the recorded throughfall (mm),  $d$  is the rain gauge diameter (of the outer rim, 20 cm), and  $A$  is the trough surface area (cm<sup>2</sup>).

## 2.4 Stemflow measurements

The selection of trees for measuring stemflow depends on a principle called the dominant tree rule. In the young forest, 3 *A. fabri* and 2 *P. purdomii* trees were selected to measure the stemflow. In the middle-aged forest, 3 *A. fabri* trees were selected to measure the stemflow. In the

mature forest, the stemflow was ignored because of its low amount (Xie et al. 2002). A hose tubing (2.0 cm in internal diameter) was bonded on top of the diameter at breast height (DBH) around the circumference of the tree trunk, which was connected and funneled into a one-tipping-bucket rain gauge to observe the stemflow. The stemflow was recorded at 1 h intervals. The stemflow depth was derived in the same way as the throughfall. The stemflow was calculated as the mean value of all the monitored trees at each plot. The stemflow depth was also derived using Eq. (1), where  $r_1$  is the recorded stemflow depth (mm) and  $A$  is the canopy area for stemflow calculation.

## 2.5 Water-holding capacity

The water-holding capacity indicates the maximum water amount that can be held by the canopy, stem, and forest litter floor, which can be defined as the saturated interception ability. Each component can be derived using the following method.

### 2.5.1. Canopy

The saturated canopy interception ( $S_c$ ) represents the capacity of canopy interception, which can be derived using the following equation (Pereira et al. 2009):

$$S_c = -\frac{b}{(\bar{E}_c/\bar{R} - 1)} \frac{\bar{E}_c}{\bar{R}} \frac{1}{\ln(1 - \bar{E}_c/\bar{R})} \quad (2)$$

where  $\bar{E}_c$  is the mean evaporation rate of the saturated canopy (mm/h) derived from the Penman–Monteith equation,  $\bar{R}$  is the mean rainfall intensity (mm/h), and  $b$  is a constant parameter (the intercept of the linear function between throughfall and rainfall), which can be given by the following equation:

$$T_f = aP_g + b \quad (3)$$

where  $T_f$  is the throughfall (mm),  $P_g$  is the gross rainfall (mm), and  $a$  is a constant parameter.

### 2.5.2. Stem

The water-holding capacity of the stem was studied by a water-spraying experiment. We chose a 100-m<sup>2</sup> study area for each forest stand. To select the trees for the experiment, the DBH, tree height, and amount of epiphytes on the trunk were considered. A total of 19 mature *A. fabri*, 25 middle-aged *A. fabri*, and 31 young *A. fabri* and *P. purdomii* were selected for the water-spraying experiment. This experiment was conducted as follows. We placed a mark on the tree bark 1.5 m above the ground. The trunk was divided into 2 sections from the mark downward along the bark. The first 0.5 m was treated as the spraying section, and the following 0.8 m was treated as the observation section. Water was sprayed along the length of the 0.5-m spraying section onto the bark, and the following 0.8-m observation section was further remarked

at 0.1 m intervals for recording. The outflow was collected using a plastic pipe around the bark at the bottom of the observation section. When the experiment was initiated, we recorded the flow lag time and the flow amount at the lower end of the observation section. All experimental data were summed to derive the average value of the saturated stem interception amount per unit area of the study stand ( $Q_{sa}$ , in cubic meters). We then obtained the total saturated stem interception at the stand scale for the different-aged forest stands using the following equation:

$$S_s = \frac{Q_{sa} \times h \times \pi \times d \times n}{A_s} \times 1000 \quad (4)$$

where  $S_s$  is the stem water-holding capacity for the study area (mm),  $h$  is the mean tree height (m),  $d$  is the mean DBH (m),  $n$  is the number of trees within the study area of  $A_s$ , and  $A_s$  is the experimental plot area (m<sup>2</sup>), which is 100 m<sup>2</sup>.

## 2.6. Forest floor litter interception capacity

Rainfall simulation experiments were conducted to evaluate the water-holding capacity of forest floor litter. Our rainfall simulator generated rainfall at the intensity of 0.35 mm/h. Forest litters were collected and then sorted according to their decomposition level. Undecomposed litter was defined as the litter that retained its original shape and properties. Half-decomposed litter was defined as partially decomposed litter with a shape that could still be distinguished. Fully decomposed litter was defined as completely decomposed litter with an indistinguishable shape. The forest litters were divided into 2 groups. The first group consisted of sorted litters with different decomposition degrees. The second group comprised the forest litter layer as a whole, such as in an in situ environment. The thickness of the litter layer, which was estimated by making random samplings at a considerable amount of points in the young, middle-aged, and mature stands, was approximately 11 cm. Forest floor litters were spread in 1-m<sup>2</sup> plastic boxes. The entire layer of forest litters was evenly spread 11 cm thick in boxes similar to the depth in the field. A polypropylene sheet was placed below the boxes at an angle of 30° and connected to the plastic drum to collect the outflow water. The remaining water was the saturated forest litter floor interception. Thus, the actual forest litter water-holding capacity was derived using the following equation:

$$S_{fl} = \frac{V_{in} - V_{out}}{A_{fl}} \times 1000 \quad (5)$$

where  $S_{fl}$  is the actual forest litter interception (mm),  $V_{in}$  is the input rainfall volume (m<sup>3</sup>),  $V_{out}$  is the outflow rainfall volume (m<sup>3</sup>), and  $A_{fl}$  is the experimental box area (m<sup>2</sup>).

Hence, the total water-holding capacity of the forest ecosystem ( $S$ ) was expressed as follows:

$$S = S_c + S_s + S_{fl} \quad (6)$$

## 2.7. $\delta^{18}\text{O}$ isotope measurements

One of the main processes that cause  $\delta^{18}\text{O}$  isotopic fractionation is the phase change in evaporation (Kubota et al. 2004). Generally, the  $\delta^{18}\text{O}$  isotopic composition of soil water is heterogeneous in catchments. The base flow is probably a much better indicator for forest floor evaporation. It can represent a relatively large scale and is easier to collect. The base flow accounted for 85.9% of the runoff in our study area (Lv 2009). The evaporation rate from the forest floor can be derived using the isotopic fractionation between the throughfall and base flow using the Rayleigh distillation equation under equilibrium conditions (Kubota et al. 2004; Lin et al. 2012).

The evaporation rate was estimated using the following equation:

$$\delta - \delta_0 = 1000(1/\alpha - 1) \times \ln f \quad (7)$$

where  $f$  is the remaining fraction of the water body (%);  $\delta$  and  $\delta_0$  are the isotopic compositions (‰) of the throughfall and stream flow, respectively; and  $f$  can be derived from Eq. (4).

$$f = \exp\left(\frac{\delta - \delta_0}{1000(1/\alpha - 1)}\right) \quad (8)$$

where  $\alpha$  is the equilibrium fractionation factor (‰) given by the following equation:

$$\ln \alpha = 1000 \times 1.137/T^2 - 0.4156/T - 2.0667/1000 \quad (9)$$

where  $T$  is the air temperature (K).

Finally, the evaporation rate from the forest floor (ER; %) was calculated as follows:

$$ER = \frac{E_s}{P} = \frac{(1-f) \cdot T_f}{P} \quad (10)$$

where  $T_f$  is the throughfall (mm),  $P$  is the rainfall (mm), and  $E_s$  is the forest floor evaporation (mm).

Throughfall and stream water samples were collected 3 times a month. The stream water was collected over 3 consecutive days when the throughfall stopped. All water samples were frozen below -10 °C before measurement. The samples were measured using a liquid water isotope analyzer (Los Gatos Research Inc., USA). The precision for  $^{18}\text{O}/^{16}\text{O}$  was 0.1‰.

## 2.8. Data analysis

ANOVA was used to test for the differences among the young, middle-aged, and mature forests. Descriptive statistics were used to calculate the averages and standard errors of the throughfall and isotope results. Data were analyzed using SPSS 13.0 (SPSS Inc., USA).

3. Results

3.1. Canopy interception

The canopy redistributes rainfall for the first time before it falls on the ground, and the canopy-intercepted rainfall evaporates to the atmosphere during rainfall and after rainfall has ceased. Broken loggers and blocked throughfall gauges resulted in several missing data values during the measurement period. For analysis accuracy, data were removed whenever an indication of blockage was present. To compare the different-aged stands, 82% of the throughfall data was used when all troughs worked. In our study area, the throughfall rates were  $76.7 \pm 1.2\%$ ,  $77.3 \pm 1.3\%$ , and  $74.7 \pm 1.5\%$  for the young, middle-aged, and mature forest stands, respectively. The throughfall had an obvious linear relationship with rainfall (Figure 1), with  $R^2$  greater than 0.98 ( $P < 0.01$ ).

Canopy interception amounted to 273.0, 244.9, and 296.5 mm for the young, middle-aged, and mature forests, which accounted for 23.3%, 20.9%, and 25.3% of the total rainfall, respectively. Canopy interception had a significant power law relationship with rainfall (Figure 2). When the rainfall amount was less than 2 mm, canopy interception sharply increased with increased rainfall. By contrast, canopy interception slowly increased with increased rainfall when the rainfall amount exceeded 2 mm. No correlation between interception loss and wind speed was found in our study (Figure 3), especially when the rainfall amount was larger than 1 mm.

3.2. Stemflow

By analyzing the stemflow observed during the same period as the throughfall, we concluded that the stemflow rate was less than 0.4% of rainfall for young and mature *A. fabri*. Hence, the stemflow can be ignored when calculating canopy interception. However, the stemflow rate was approximately  $1.82 \pm 0.2\%$  of rainfall in the middle-aged stand, and so it should be included in the canopy interception calculation. The annual mean relative humidity was approximately 90%. Epiphytes can grow

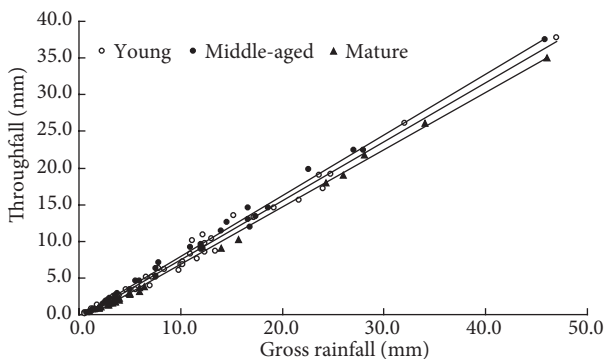


Figure 1. Relationship between throughfall and gross rainfall for the 3 forest types ( $R^2 = 0.9926$ ,  $0.9831$ , and  $0.9941$  for the young, middle-aged, and mature forests, respectively).

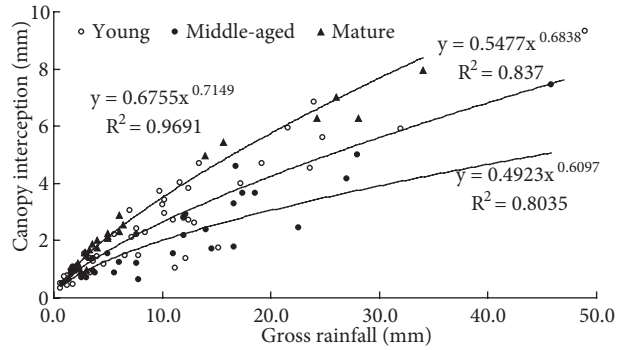


Figure 2. Relationship between canopy interception and gross rainfall for the 3 forest types. The young and middle-aged interceptions were measured, and the mature interception was derived from literature. A power function between gross rainfall and canopy interception is shown. For young: ,  $R^2 = 0.837$ ; for middle-aged: ,  $R^2 = 0.8035$ ; for mature: ,  $R^2 = 0.9691$ .

very well on Gongga Mountain, with a coverage rate of approximately 85% on a tree's trunk, branches, and stems. The epiphyte thickness was approximately 2.0 cm. A considerable amount of water that flows down the stems can be absorbed. This phenomenon was the main reason for the very small amount of stemflow in the young forest stand.

3.3. Forest floor interception

The throughfall can be reintercepted by forest litters in a process similar to that of canopy interception. The intercepted water then returns to the air during evaporation. Forest litters can also prevent soil erosion due to raindrop impacts. The ratio of the forest floor evaporation to the gross rainfall was calculated using isotope methods. In different months (from May to October),  $f$  ranged from 92.3% to 97.8%, 93.2% to 96.7%, and 95.2% to 98.7% for the young, middle-aged, and mature forest, respectively. Based on Eq. (10) and the throughfall data, the forest floor evaporation amounted to 78.6, 65.7, and 44.3 mm for the young, middle-aged, and mature forest, respectively (Table 2). The remaining water in

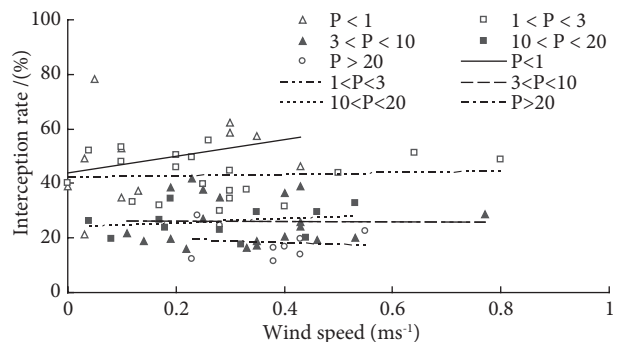


Figure 3. Relationship between wind speed and canopy interception rate. The wind speed is the mean value over a rainfall event ( $m s^{-1}$ ).  $P$  is the gross rainfall (mm).

**Table 2.** Results of the calculation of forest floor litter evaporation using the isotope method. The standard deviation of  $f$  represents the variation in different months (from May to October 2009).  $f$  is the remaining fraction of the water body,  $E_s$  is the soil evaporation, and  $ER$  is the rate of evaporation from the forest floor to  $P_g$ .

	$f$ (%)	$E_s$ (mm)	$ER$ (%)
Young	96.03 ( $\pm 1.22$ )	78.6	5.48
Middle-aged	95.05 ( $\pm 1.81$ )	65.7	4.62
Mature	97.05 ( $\pm 1.12$ )	44.3	3.07

the soil then became runoff or returned to the atmosphere via transpiration.

**3.4. Water-holding capacity**

During the study period,  $\bar{R}$  was 0.96 mm/h and  $\bar{E}_c$  was 0.055 mm/h. Based on Eq. (2), we can obtain the saturated canopy interception values, which were 1.23 and 1.21 mm for the young and middle-aged stands, respectively. Mature *A. fabri* had a larger saturated canopy interception (3.15 mm) because of its luxuriant foliage and spreading branches. An alternative method to estimate  $S$ , i.e. by analyzing the rainfall events that both saturated and unsaturated the canopy, was illustrated using young *A. fabri* (Klaassen et al. 1998). The canopy water-holding capacity obtained by this method was 1.5 mm (Figure 4), which was a little higher than that calculated by Eq. (2).

The stem interception capacity was about 1.33 mm for the young and middle-aged forest stands. The stem interception of the mature *A. fabri* stand was 0.81 mm when only live trees were considered in the calculation. Field investigations revealed that a considerable number of dead trees, also called coarse woody debris, still stand in the mature forest site. The stem interception capacity of the dead stand trees was 3 times that of live ones because the dead stand's woody trunk can absorb more water than

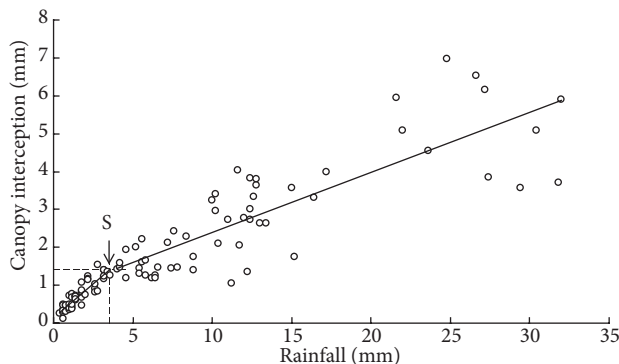


**Figure 4.** Canopy interception versus rainfall for all rainfall events in the young forest between May and October 2009.  $S$  is the saturated canopy interception capacity (approximately 1.5 mm) as determined from a fit on observations.

the live stand's. Therefore, the mature forest had the largest stem interception capacity, 2.56 mm, when dead stand trees were considered.

The experimental results showed that the forest litter water-storage capacity varied with the decomposition level (Figure 5). The fully decomposed litter had the maximum potential rainfall interception capacity, whereas the undecomposed litter had the minimum capacity. We concluded that the fully decomposed litter had larger porosities; thus, its water-holding capacity was relatively larger. Undecomposed litter comprised leaves and branches that had existed on the forest floor for a relatively shorter time. These leaves and branches had smaller porosities and thus cannot hold large amounts of water. The water-holding capacity also varied with the forest stand. The young stand exhibited the largest water-holding capacity for all 3 decomposition levels. For the entire forest litter layer experimental scheme, the water-holding capacities were 5.66, 5.07, and 5.07 mm for the young, middle-aged, and mature stands, respectively.

**3.5. Total interception**

The water-storage capacity was the main component of interception. According to the experimental results, the young, middle-aged, and mature forest types can hold 8.22, 7.61, and 10.78 mm of water, respectively (Figure 6), which still evaporated after rain had ceased.

The results showed that the total interceptions were 411.6, 364.5, and 444.5 mm for the young, middle-aged, and mature forests, respectively. The mature forest exhibited the largest interception capacity. The components of total interception are shown in Figure 7. The canopy interception accounted for 80.9%, 81.9%, and 90.0% of total interception for the young, middle-aged, and mature forest types, respectively. Forest floor interception also had a significant contribution to the total interception. The total interception ratio increased with LAI, similar to the canopy interception (Figure 8). In contrast, the forest floor

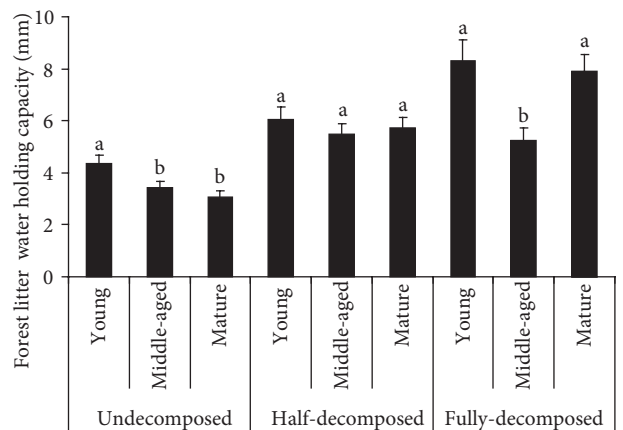


**Figure 5.** Forest litter water-holding capacity under the different decomposition conditions.

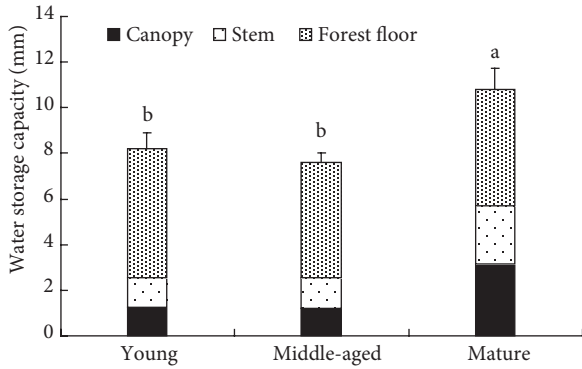


Figure 6. Water-storage capacity of the different forest types.

interception showed an inverse relationship with LAI. However, the middle-aged forest with a smaller LAI had a larger forest floor interception ratio relative to the young forest. The result indicated that the forest height may also prevent water from evaporating from the forest floor.

#### 4. Discussion

##### 4.1. Canopy interception

Despite thorough cleaning every 2 weeks, the throughfall troughs were still blocked by fallen leaves or twigs. Blockage was identified by examining the changes in the throughfall response to rainfall and comparing with other gauges. In our research, the canopy interception rates were 23.3%, 20.9%, and 25.3% for the young, middle-aged, and mature *A. fabri*, similar to the mean value for global needle-leaved forests (Miralles et al. 2010). The difference among the canopy interceptions of the different-aged *A. fabri* was probably caused by variations in the LAI. Globally, a canopy cover increases from pioneer to late-successional stages for natural forests (Howard and Lee 2003). In our study area, the LAI of the young forest was much larger than that of the middle-aged forest. LAI generally increased with increased precipitation, and also correlated with soil organic carbon as well as total nitrogen

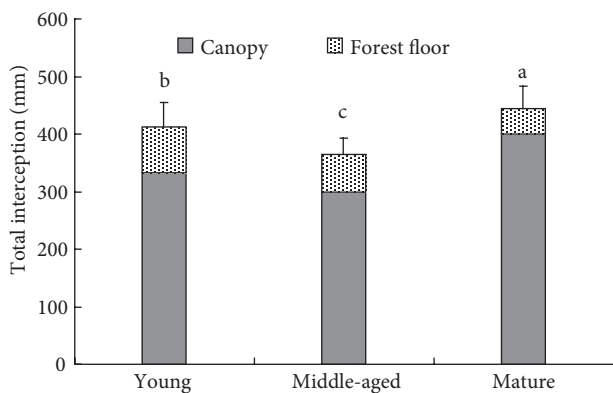


Figure 7. Total interception and its components for the young, middle-aged, and mature forest types.

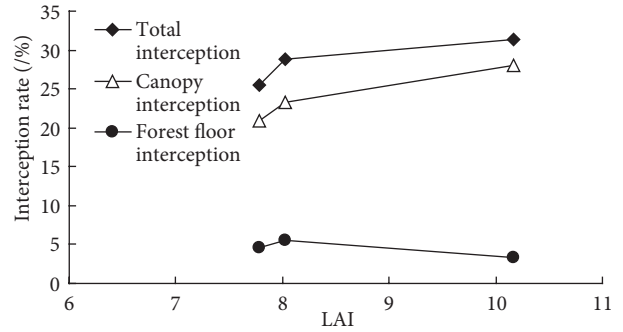


Figure 8. Relationship between the interception rates of the different components and LAI.

contents of Mt. Gongga (Luo et al. 2004). Larger canopy storage resulted in a larger canopy interception loss under relatively similar climatic conditions. The night rainfall rate was approximately 66.0%. The rainfall intercepted at night and then evaporated the following day, and the dry canopy reintercepted rainfall in the next rainfall event (Lin et al. 2012).

Theoretically, strong wind conditions are associated with less interception loss (Höermann et al. 1996). However, with the high canopy density in tropical rain forests, strong winds can generate high interception loss rates (Herwitz and Slye 1995). The same phenomenon has been reported in boreal and temperate forests (Toba et al. 2005). No apparent correlation between interception loss and wind speed was found in our study (Figure 3). On Gongga Mountain, the mean wind speed was 0.39 m/s, and canopy interception was barely influenced by the wind due to the hardness of the branch/twig/leaf. Canopy interception was sensitive to the rainfall amount, rainfall duration, and rainfall intensity (Miralles et al. 2010). The rainfall events in our study were mainly long-duration, low-intensity synoptic events. We can conclude that canopy interception was significantly correlated with the rainfall amount, i.e. the controlling factor for canopy interception was the rainfall characteristic (Figure 2).

##### 4.2. Stem interception

The stemflow is an important process that affects the biogeochemical cycling of nutrients within and through forests (Levia and Frost 2003). Our research demonstrated that the stemflow rate was less than 1% of the gross rainfall. A similar result was obtained from Chinese fir and Faber fir-spruce forest. The stemflow was lower under coniferous than under broadleaf forests (Barbier et al. 2009). Coniferous species have a stemflow-reducing “funnel crown” (Otto 1998). Rough bark and epiphytes may also play important roles in determining the stemflow in our study.

The water-storage capacity of epiphytes depends on their biomass (Köhler et al. 2007). The young forest’s

larger water-storage capacity may be due to the greater epiphyte biomass with high density. The epiphyte storage of the young and middle-aged forest was a little larger compared with the canopy storage (Figure 5). Hölischer et al. (2004) found that although the water-storage capacity of an epiphyte was close to that of the canopy, the epiphyte contributed only approximately 6% of the modeled total interception. The main reason was that the epiphyte was usually close to saturation during the rainy season. Hence, the effective water-storage capacity was much lower than the potential value. We also found this phenomenon in the subalpine Gongga Mountain forests. The epiphytes were always wet because the most of the epiphytes grew in the shadowed areas where the evaporation rates were low (Veneklaas et al. 1990). This phenomenon demonstrated that the interception capacity of the epiphyte was significant, but the stem interception contribution to the total interception was limited.

#### 4.3. Forest floor interception

The hydraulic mechanisms of the forest floor interception are similar to that of the canopy interception process. The amount of rainfall intercepted by the forest floor is related to the water-storage capacities of the surface components (Putuhena and Cordery 1996), which have high spatial variability. The observed spatial patterns in the forest floor water content are inconsistent over time. Stable isotopes

are demonstrated to be an effective method to study forest floor evaporation (Kubota et al. 2004), but the result can be influenced by preferential flow. Niu et al. (2007) reported that the Gongga Mountain ecosystem had preferential flow phenomenon. To avoid the effect of preferential flow on estimating forest floor evaporation, stream water was collected for 3 consecutive days after the throughfall stopped. Stream water samples during and after the new rainfall events were also excluded to avoid the mixing effect of an isotope (Lin et al. 2012). Thus, we concluded that the ratio of the forest floor evaporation determined by isotopes was reliable in our study.

Previous studies on the forest floor water-storage capacity are summarized in Table 3.  $S_{ff}$  in our study was within the range of the rainfall forest, but a little higher than the other forest types. Despite the vegetation types, the forest floor interception has a linear relationship with the thickness of forest litter (Putuhena and Cordery 1996; Marin et al. 2000). A similar conclusion was obtained in the upper reaches of the Yangtze River (Shi et al. 2004), the region where Gongga Mountain is located.

The rate of the forest floor interception to the throughfall was less than 7.7% in our study, and the rate decreased with increased stand age. The results of a previous study on the forest floor interception ratio are shown in Table 4. Our result was between that of Japanese

**Table 3.** Forest floor storage capacity for the different vegetation types.

Vegetation	Forest floor storage capacity (mm)	Source
Beech	1.8	Gerrits et al. (2010)
<i>Pinus radiata</i>	2.8	Putuhena et al. (1996)
Sclerophyll eucalypt	1.7	Putuhena et al. (1996)
Deciduous forest	2.0	Wilson et al. (2000)
Rain forest	4.57–16.29	Marin et al. (2000)

**Table 4.** Rates of evaporation from the forest floor to the gross rainfall in previous studies.

Vegetation	Rate (%)	Source
Japanese cypress, Japanese cedar	3.5–9.1	Kubota et al. (2004)
Global scale	4.3	Miralles et al. (2011)
Savannah	16.0	Tsiko et al. (2012)
Beech	22.0	Gerrits et al. (2010)
<i>Dacrydium cupressinum</i>	5.3	Barbour et al. (2004)
Rain forest	7.0–13.0	Marin et al. (2000)

cypress and Japanese cedar derived by stable isotopes (Kubota et al. 2004) and an energy balance approach (Marin et al. 2000; Barbour et al. 2005), but lower than a previous result obtained by continuous weight measuring experiment (Gerrits et al. 2010; Tsiko et al. 2012). The soil layer is thin on Mt. Gongga. The deeper layer is accompanied by much detrital rock, and the organic matter content is high in the superficial layer. The soil steady permeability is 8.0–11.0 mm/min, which is larger than the rainfall density (Zhang et al. 2004). Due to the high rainfall amount and low temperature, the forest floor was always wet from May to October. We concluded that the lower ratio of the forest floor interception may be due to the lower incoming net radiation and low wind speed. Wang et al. (2004) demonstrated that the canopy may play a role in controlling the energy partition between the overstory and understory layers, and that the net radiation absorption ratio of the forest floor to the canopy in a pine forest was less than 0.47. The net radiation absorption ratio decreased with increased LAI. Wilson et al. (2000) also found that the net radiation at the forest floor is 21.5% of that above the canopy, and the fluxes from the forest floor are roughly 15%–22% of those above the canopy.

The forest floor evaporation ratio decreased with increased stand age in our study area. Two controlling factors may contribute to this phenomenon. On one hand, the LAI determined the rate of forest floor evaporation. On the other hand, the height of the different stands may be accountable. Lower stands gave better ventilation to the forest floor; thus, the rates of forest floor evaporation were higher. Kubota et al. (2004) found that a mature forest had a larger water loss than a young forest. Tsiko et al. (2012) suggested that canopy coverage and wind are the

factors that induced the discrepancy among interception evaporation results.

The results of this study showed the importance of interception. The stand age significantly influenced the interception in our study area. During the study period, the total interception rates were 28.8%, 25.5%, and 31.1% for the young, middle-aged, and mature *A. fabri*, whereas the canopy water-storage capacities were 1.23, 1.21, and 3.15 mm, respectively. The stem water-storage capacity varied from 1.33 mm for the young and middle-aged forest to 0.81 mm for the mature forest, whereas the forest floor water-storage capacity ranged from 5.66 mm for the young forest to 5.07 mm for both the middle-aged and mature forests. Although the sum of the stem and forest floor water-storage capacities was larger than that of the canopy, the dominant component of interception was canopy interception. The forest floor interception had only a limited contribution of less than 19.1% to interception and it decreased with increased stand age. For the canopy interception of a particular forest type, the characteristics of the rainfall were the controlling factors, whereas wind apparently had no impact. Evaporation from stem and forest floor interceptions was low due to the higher aerodynamic and surface resistances.

### Acknowledgments

This study was funded by the National Natural Science Foundation Committee (40730634) and the Knowledge Innovation Project of the Chinese Academy of Sciences (KZCX2YW-331). We also thank every member of the project for their hard work in the in situ experiments. The constructive criticism of all reviews and editors on this paper was much appreciated.

### References

- Barbier S, Balandier P, Gosselin F (2009) Influence of several tree traits on rainfall partitioning in temperate and boreal forests: a review. *Ann For Sci* 66: 602.
- Barbour MM, Hunt JE, Walcroft AS, Rogers GND, McSeveny TM, Whitehead D (2005) Components of ecosystem evaporation in a temperate coniferous rainforest, with canopy transpiration scaled using sapwood density. *New Phytol* 165: 549–558.
- Blyth E, Harding RJ (2011) Methods to separate observed global evapotranspiration into the interception, transpiration and soil surface evaporation components. *Hydrol Process* 25: 4063–4068.
- David TS, Gash JHC, Valente F, Pereira JS, Ferreira MI, David JS (2006) Rainfall interception by an isolated evergreen oak tree in a Mediterranean savannah. *Hydrol Process* 20: 2713–2726.
- Fleischbein K, Wilcke W, Goller R, Boy J, Valarezo C, Zech W, Knoblich K (2005) Rainfall interception in a lower montane forest in Ecuador: effects of canopy properties. *Hydrol Process* 19: 1355–1371.
- Gash JHC, Wright IR, Lloyd CR (1980) Comparative estimates of interception loss from three coniferous forests in Great Britain. *J Hydrol* 48: 89–105.
- Gerrits AMJ, Pfister L, Savenije HHG (2010) Spatial and temporal variability of canopy and forest floor interception in a beech forest. *Hydrol Process* 24: 3011–3025.
- Hattori S (1983) The seasonal variation of evaporation from forest floor in a hinoki stand. *J Jpn For Soc* 65: 9–16.
- Helvey JD (1967) Interception by eastern white pine. *Water Resour Res* 3: 723–729.
- Herwitz SR, Slye RE (1995) Three-dimensional modeling of canopy tree interception of wind-driven rainfall. *J Hydrol* 168: 205–226.
- Hörmann G (1996) Calculation and simulation of wind controlled canopy interception of a beech forest in Northern Germany. *Agr For Meteorol* 79:131–148.
- Hölscher D, Köhler L, Albert IJM, Bruijnzeel LA (2004) The importance of epiphytes to total rainfall interception by a tropical montane rain forest in Costa Rica. *J Hydrol* 292: 308–322.

- Howard LF, Lee TD (2003) Temporal patterns of vascular plant diversity in southeastern New Hampshire forests. *For Ecol Manage* 185: 5–20.
- Johnson RC (1990) The interception, throughfall and stemflow in a forest highland in Scotland and the comparison with other upland forests in the UK. *J Hydrol* 118: 281–287.
- Klaassen W, Bosveld F, Water E (1998) Water storage and evaporation as constituents of rainfall interception. *J Hydrol* 212–213: 36–50.
- Köhler L, Tobon C, Frumau KFA (2007) Biomass and water storage dynamics of epiphytes in old-growth and secondary montane cloud forest stands in Costa Rica. *Plant Ecol* 193: 171–184
- Kubota T, Tsuboyama Y (2004) Estimation of evaporation rate from the forest floor using oxygen-18 and deuterium compositions of throughfall and stream water during a non-storm runoff period. *J For Res* 9: 51–59.
- Lawrence DM, Thronton PE, Olsen KW, Bonan GB (2007) The partitioning of evapotranspiration into transpiration, soil evaporation, and canopy evaporation in a GCM: impacts on land-atmosphere interaction. *J Hydrometeorol* 8(7): 862–880.
- Levia DE, Frost EE (2003) A review and evaluation of stemflow literature in the hydrologic and biogeochemical cycles of forested and agricultural ecosystems. *J Hydrol* 274: 1–29.
- Lin Y, Wang GX, Guo JY, Sun XY (2012) Quantifying evapotranspiration and its components in a coniferous subalpine forest in southwest China. *Hydrol Process* 26: 3032–3040.
- Luo TX, Pan YD, Ouyang H, Shi PL, Luo J, Yu ZL, Lu Q (2004) Leaf area index and net primary productivity along subtropical to alpine gradients in the Tibetan Plateau. *Glob Ecol Biogeogr* 13: 345–358.
- Lv YX (2009) Runoff characteristics analysis of different small basins in Hailuoguo River. MS Thesis. Institute of Mountain Hazards and Environment, Chinese Academy of Sciences, Chengdu, China.
- Mair A, Fares A (2010) Throughfall characteristics in three non-native Hawaiian forest stands. *Agric For Meteorol* 150: 1453–1466.
- Marin CT, Bouten IW, Dekker S (2000) Forest floor water dynamics and root water uptake in four forest ecosystems in northwest Amazonia. *J Hydrol* 237: 169–183.
- Merta M, Seidler C, Fjodorowa T (2006) Estimation of evaporation components in agricultural crops. *Bio Bratisl* 61: S280–S283.
- Miralles DG, De Jeu RAM, Gash JHC, Holmes TRH, Dolman AJ (2011) Magnitude and variability of land evaporation and its components at the global scale. *Hydrol Earth Syst Sci* 15: 967–981.
- Miralles DG, Gash JHC, Holmes TRH (2010) Global canopy interception from satellite observations. *J Geophys Resour* 115: D16122.
- Murakami S, Tsuboyama Y, Shimizu T, Fujieda M, Noguchi S (2000) Variation of evapotranspiration with stand age and climate in a small Japanese forested catchment. *J Hydrol* 227: 114–127.
- Niu JZ, Yu XX, Zhang ZQ (2007) Soil preferential flow in the dark coniferous forest of Gongga Mountain based on the kinetic wave model with dispersion wave (KDW preferential flow model). *Acta Ecol Sin* 27: 3541–3555.
- Otto HJ (1998) *Écologie forestière*, Institut pour le Développement Forestier, Paris.
- Pereira FL, Gash JHC, David JS, David TS, Monteiro PR, Valente F (2009) Modelling interception loss from evergreen oak Mediterranean savannas: application of a tree-based modeling approach. *Agric Forest Meteorol* 149: 680–688.
- Putuhena WM, Cordery I (1996) Estimation of interception capacity of the forest floor. *J Hydrol* 180: 283–299.
- Pypker TG, Unsworth MH, Bond BJ (2006) The role of epiphytes in rainfall interception by forests in the Pacific Northwest. II. Field measurements at the branch and canopy scale. *Can J For Res* 36: 819–832.
- Rowe LK (1983) Rainfall interception by an evergreen beech forest, Nelson, New Zealand. *J Hydrol* 66: 143–158.
- Rutter AJ, Morton AJ, Robins PC (1975) A predictive model of rainfall interception in forest. II. Generalization of the model and comparison with observation in some coniferous and hardwood stands. *J Appl Ecol* 12: 367–380.
- Savenije HHG (2004) The importance of interception and why we should delete the term evapotranspiration from our vocabulary. *Hydrol Process* 18: 1507–1511.
- Schellekens J, Bruijnzeel LA (2000) Evaporation from a tropical rain forest, Luquillo Experimental Forest, eastern Puerto Rico. *Water Resour Res* 36: 2183–2196.
- Shi PL, Wu B, Cheng GW, Luo J (2004) Water retention capacity evaluation of main forest vegetation types in the upper Yangtze basin. *J Nat Resour* 19: 352–359.
- Shuttleworth WJ (1992) Evaporation. In: *Handbook of Hydrology* (Ed. D. Maidment). McGraw-Hill, New York, pp. 4.1–4.53.
- Tajchman SJ (1972) The radiation and energy balances of coniferous and deciduous forests. *J Appl Ecol* 9: 357–375.
- Toba T, Ohta T (2005) An observational study of the factors that influence interception loss in boreal and temperate forests. *J Hydrol* 313: 208–220.
- Tsiko CT, Makurira H, Gerrits AMJ, Savenije HHG (2012) Measuring forest floor and canopy interception in a savannah ecosystem. *Phys Chem Earth* 47–48: 122–127.
- Veneklaas EJ, Van ER (1990) Rainfall interception in two tropical montane rain forests, Colombia. *Hydrol Process* 4: 311–326.
- Vertessy RA, Watson FGR, O'Sullivan SK (2001) Factors determining relations between stand age and catchment water balance in mountain ash forests. *For Ecol Manage* 143: 13–26.
- Wang KY, Kellomäki S, Zha TS, Peltola H (2004) Seasonal variation in energy and water fluxes in a pine forest: an analysis based on eddy covariance and an integrated model. *Ecol Model* 179: 259–279.
- Wilson KB, Hanson PJ, Baldocchi DD (2000) Factors controlling evaporation and energy partitioning beneath a deciduous forest over an annual cycle. *Agric For Meteorol* 102: 83–103.
- Xie CH, Guan WB, Wu JA, Cheng GW, Luo J (2002) Interception capacity of dark coniferous forest ecosystem in Gongga Mountain. *J Beijing For Univ* 24: 68–71.
- Zhang BH, He YR, Zhou HY, Cheng GW (2004) Water characteristics and its eco-environmental effects on soils under different subalpine forests on east slope of Gongga Mountain. *J Mt Sci* 22: 207–211.